Numerical study on behaviors of vertically-loaded Tender Net Foundations supported by piles

Han Vo-Cong
Takeuchi Construction Inc., Hiroshima, Japan. E-mail: han@takeuchi-const.co.jp

Kinji Takeuchi
Takeuchi Construction Inc., Hiroshima, Japan. E-mail: takeuchi@takeuchi-const.co.jp

Yasuo Tomono
Takeuchi Construction Inc., Hiroshima, Japan. E-mail: tomonou@takeuchi-const.co.jp

Tatsunori Matsumoto
Kanazawa University, Ishikawa, Japan. E-mail: matsumototatsunori55@gmail.com

Keywords: TNF system, soil improvement, piled raft foundation, vertical load, FEM, load sharing

ABSTRACT: Tender Net Foundation (TNF), a kind of shallow foundation with soil improvement, has been developed for foundations of low-rise buildings on soft grounds. In the TNF, a grid-shaped soil improvement layer works as the raft foundation instead of the usual raft of reinforced concrete. The TNF is an efficient foundation to reduce the vertical displacements and volume of soil improvement compared to normal raft foundations. In this paper, numerical analyses of behaviors of TNFs supported by piles (Piled TNF) on very soft ground are carried out aiming at reducing differential displacement as well as average displacement. First, a FEM analysis of the TNF alone (Unpiled TNF) is conducted to estimate the vertical load-displacement relation to confirm that the bearing capacity is secured for vertical load of a 5-story (mid-rise) building. Then, FEM analyses of Piled TNFs supported by various combinations of pile diameters, lengths, numbers, and arrangements are conducted.

1. INTRODUCTION

Tender Net Foundation (TNF system), a kind of shallow foundation with soil improvement, has been developed for foundations of low-rise buildings on soft grounds. In the TNF system, as shown in Fig. 1 and Fig. 2, a grid-shaped soil improvement layer works as the raft foundation instead of the usual raft of reinforced concrete. In the TNF system, the soft ground is improved to depths of 2 to 3 m usually.

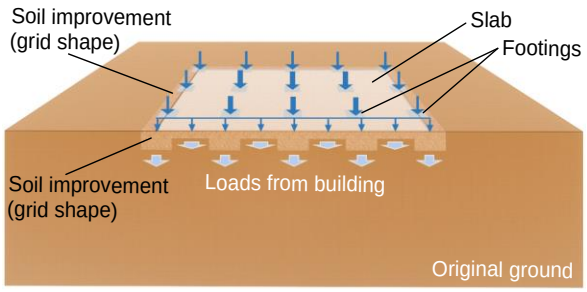

Figure 1. Section view of a TNF system

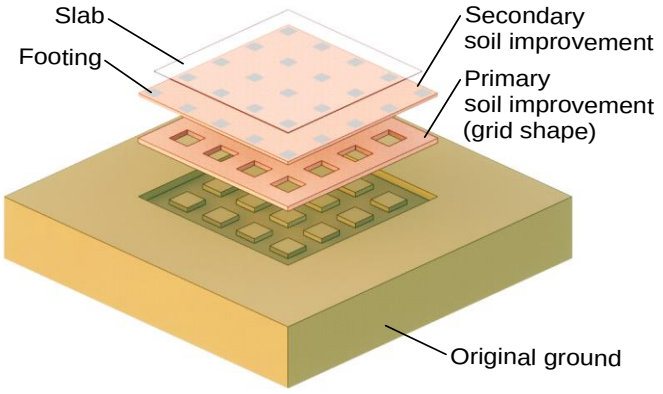

Figure 2. Composition of a TNF system

Cong et al. (2022) analyzed the TNF system in the cases of the low-rise building constructed on soft ground with various stiffness. Cong et al. (2022) demonstrated that the TNF system is an efficient foundation for reducing the settlement and volume of soil improvement compared to normal raft foundations.

In this paper, numerical analyses on behaviors of vertically loaded TNFs supported by piles (Piled TNF) on very soft ground are carried out aiming at reducing differential vertical displacements as well as average displacement.

First, FEM analysis of the TNF system alone (Unpiled TNF) is conducted to estimate the vertical load-displacement relation to confirm that the bearing capacity is secured for the vertical load of a 5-story (mid-rise) building. Then, FEM analyses of Piled TNFs supported by various combinations of pile diameters, lengths, numbers, and arrangements are conducted.

2. FEM ANALYSIS OF VERTICAL LOAD-DISPLACEMENT RELATION OF UNPILED TNF

2.1 Analysis conditions

Fig. 3 shows the detailed configuration of a typical TNF system with a primary soil improvement of 1.5 m thick having the grid shape and a secondary soil improvement of 1.0 m thickness. The dimensions of other parts are also shown in Fig. 3.

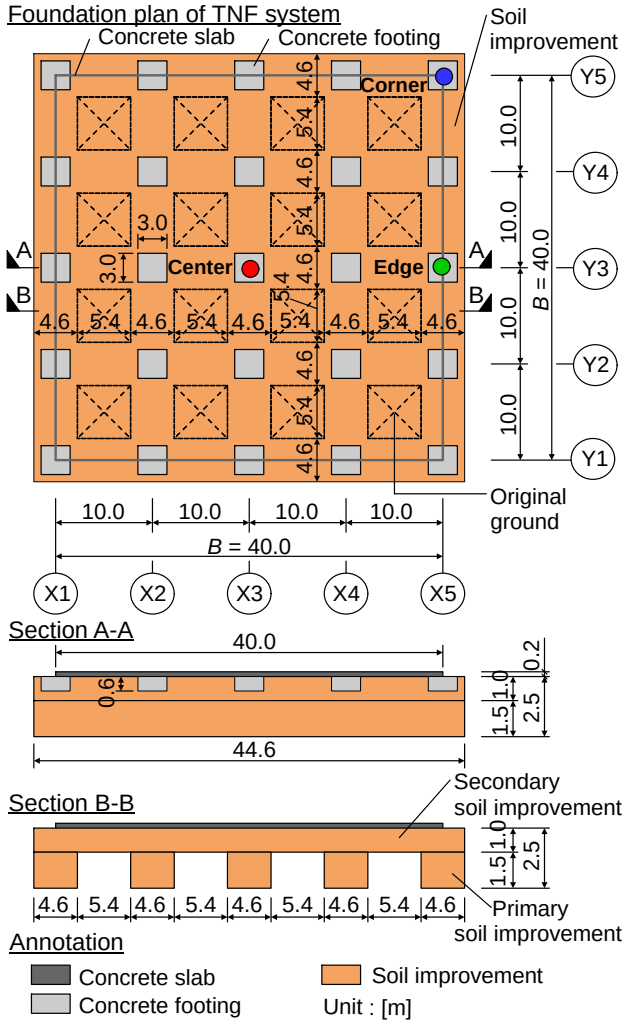

Figure 3. Configuration of the TNF system

The PLAXIS 3D FEM software (Bentley, 2022) was used for the analyses.

Fig. 4 shows the FEM analysis model with the load conditions of a 1-story building.

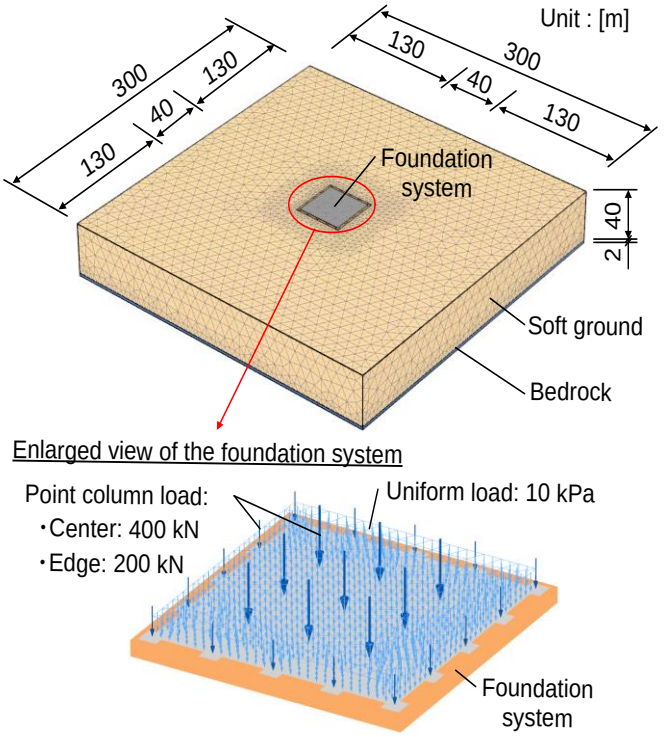

Figure 4. FEM analysis model

To obtain vertical load-displacement relation of the Unpiled TNF system, vertical loads from the building are applied to the TNF system considering loads of 1-story to 35-story buildings. Specifically, the uniform load of 10 kPa on the ground floor is applied to the slab as shown in Fig. 4. The uniform load of 0.8 kPa on the upper floors is converted to column loads.

In this analysis, the parameters of the ground and each part of the foundation system are listed in Tables 1, 2, 3, and 4.

It is assumed that a very soft ground having a constant undrained shear strength of 20 kPa exists to a depth of 40 m underlain by a hard bedrock. This extreme modeling was made for the purpose of studying the behavior and determining the bearing capacity of the TNF system in the worst ground condition.

For the first step of research, a simple but workable soil model, Mohr-Coulomb model, was selected.

Although the undrained shear strength c_u was used for the failure criterion, the fully-drained condition of the ground was assumed to avoid underestimation of the displacements of the ground and the foundation. That is, safety side analyses were conducted in this paper.

Table 1 Mechanical and physical parameters of the soft ground (Mohr-Coulomb model)

Parameter	Value
Young's modulus, E_s (kPa)	2,350
Poisson's ratio, v	0.2
Unit weight, γ (kN/m^3)	16
Undrained shear strength, c_u (kPa)	20
Internal friction angle, ϕ (deg.)	0

Table 2 Mechanical and physical parameters of the bedrock (Linear elastic model)

Parameter	Value
Young's modulus, E_b (kPa)	168,000
Poisson's ratio, v	0.2
Unit weight, γ (kN/m^3)	20

Table 3 Mechanical and physical parameters of the soil improvement of the TNF system (Mohr-Coulomb model)

Parameter	Value
Young's modulus, E_1 (kPa)	81,000
Poisson's ratio, v	0.2
Unit weight, γ (kN/m^3)	17
Undrained shear strength, c_u (kPa)	225
Internal friction angle, ϕ (deg.)	0

Table 4 Mechanical and physical parameters of the concrete (Linear elastic model)

Parameter	Value
Young's modulus, E_c (kPa)	23.5×10^6
Poisson's ratio, v	0.2
Unit weight, γ (kN/m^3)	24

E_1 in Table 3 is defined as the secant modulus E_{50} by Eq. (1) specified in the Building Center of Japan (2018).

$$E_{50} = 180 \times F_c \quad (1)$$

where F_c is the unconfined compression strength of the soil improvement (F_c = 450 kPa).

The Building Center of Japan (2019) specifies the empirical equation (2) to estimate Young's modulus E of the original ground from SPT N-value.

$$E = 2800\,N \text{ (kPa)} \quad (2)$$

In this series of analyses, N-value was assumed to be 0.8 for E_s of soft ground in Table 1 and 60 for E_b of bedrock in Table 2.

2.2 Analysis results

Fig. 5 shows the calculated deformation of Unpiled TNF due to the vertical loads of the 5-story building. The foundation system has a dish shape due to the vertical loading. The maximum vertical displacement occurs at the center point and the displacement gradually decreases towards the corner and the edges of the foundation system.

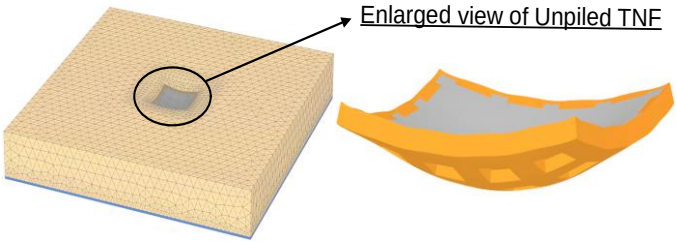

Figure 5. Calculated deformation of Unpiled TNF due to vertical loads of 5-story building

Fig. 6 shows the calculated vertical load-displacement curves at the three points of the center, edge, and corner of the slab (Fig. 3).

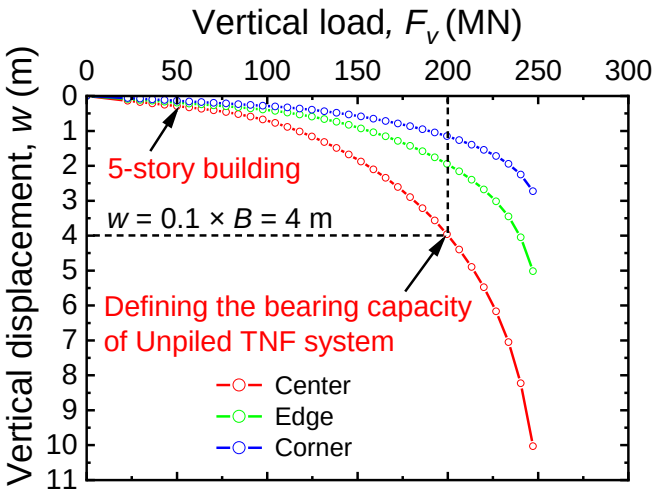

Figure 6. Calculated vertical load-displacement curves of the Unpiled TNF

It is seen from Fig. 6 that for vertical load F_v less than about 70 MN, the vertical load-displacement curves are nearly linear. Meanwhile, for F_v greater than about 70 MN, the vertical load-displacement curves are non-linear.

In this paper, the bearing capacity Q of the Unpiled TNF was defined as the F_v at the displacement of 4.0 m (0.1×B) following Briaud and Jeanjean (1994) at the center (Q = 200 MN).

Fig. 7 shows the failure zones (red color) of the ground at F_v = 50 MN (5-story) and F_v = 84 MN (10-story). The failure zone of an inverse pyramid shape develops under the Unpiled TNF at F_v = 84 MN (Fig. 7b). On the other hand, the failure zones of the ground are minor at F_v = 50 MN, as shown in Fig. 7a.

Even at F_v = 50 MN, a maximum displacement of 291 mm and a differential displacement of 154 mm occurred, resulting in excessive deformation of the foundation.

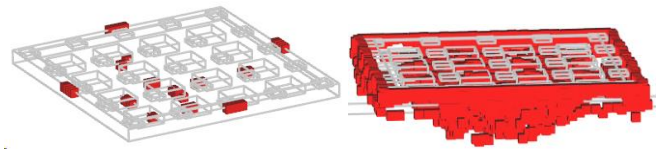

(a) F_v = 50 MN (5-story) (b) F_v = 84 MN (10-story)

Figure 7. Failure points (zone) of the ground

3. NUMERICAL ANALYSES OF PILED TNF

3.1 Analysis conditions

In this section, the performance of Piled TNFs (Fig. 8) is investigated numerically for the reduction of differential displacement as well as average displacement.

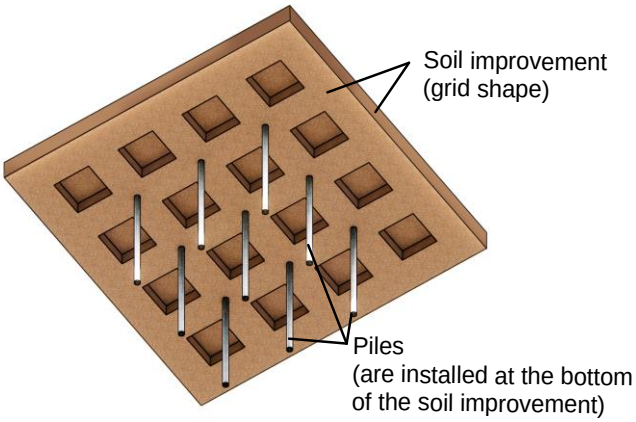

(a) n = 9

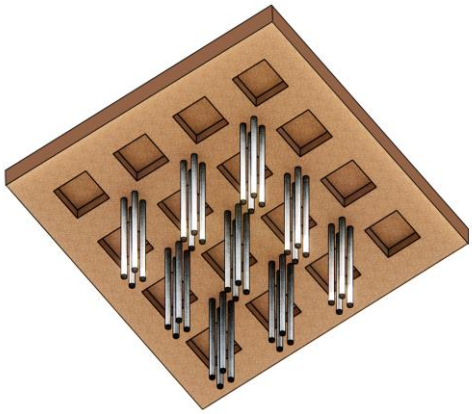

(b) n = 9 × 4

Figure 8. Bottom view of examples of Piled TNF

Table 5 shows the mechanical and geometrical properties of the piles used in the analyses. The parameters of the ground and each part of the foundation system were listed in Tables 1, 2, 3, and 4 in Section 2.1.

"Embedded beam (pile)" prepared in PLAXIS 3D was employed for modeling piles. For embedded piles, the shaft resistance τ_f and the toe resistance q_p should be assigned.

Table 5 Mechanical and geometrical properties of the piles

Parameter	Value
Young's modulus, E (kPa)	40×10^6
Poisson's ratio, ν	0.2
Unit weight, γ (kN/m^3)	24
Outer diameter, D (m)	0.40 ~ 1.00
Inner diameter, d (m)	0.27 ~ 0.74
Length, L (m)	20 ~ 40

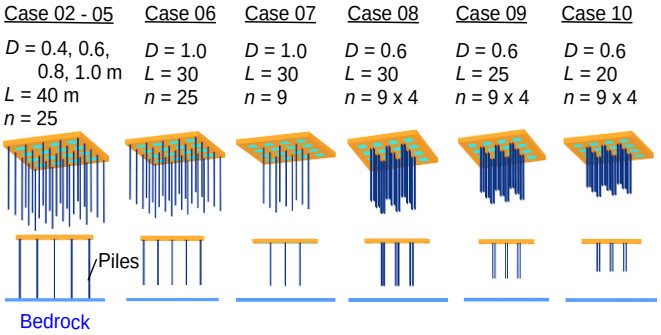

Figure 9. Analysis cases

In the numerical analyses, diameter D, length L, number of piles n, and arrangements were varied as shown in Fig. 9. The piles were set beneath the primary soil improvement layer below the concrete footings. The vertical load of the 5-story building described in Section 2.1 was applied in all the cases.

Case 01 is the TNF system without piles (Unpiled TNF). Cases 02 to 05 are four cases of the TNF system supported by piles reaching the bedrock (namely, end-bearing pile cases). The embedment length into the bedrock is 1.5 m. Cases 06 to 10 are five cases of the TNF system supported by friction piles (friction pile cases). Case 06 is a fully piled TNF where 25 piles are arranged evenly beneath the whole area of the TNF. Meanwhile, Cases 07, 08, 09, and 10 are the TNF system supported by small centered friction pile groups. In Case 07, one large-diameter pile (D = 1.0 m) is arranged below nine concrete footings. In Cases 08, 09, and 10, four slender piles (D = 0.6 m) are arranged below nine concrete footings.

Maximum shaft resistance τ_f of the embedded piles was set to be 20 kPa which is equal to the undrained shear strength c_u of the ground.

In friction pile cases, the pile toe resistance q_p was set as zero conservatively.

In end-bearing pile cases, q_p was estimated by Eq. (3) (The Building Center of Japan, 2019).

$$q_p = 150 \times N \text{ (kPa)} \quad (3)$$

N = 60 was assumed for the bedrock.

3.2 *Analysis results*

Fig. 10 shows the plan view of Piled TNF and the arrangement of piles in Cases 08 to 10 (n = 9 × 4) for example.

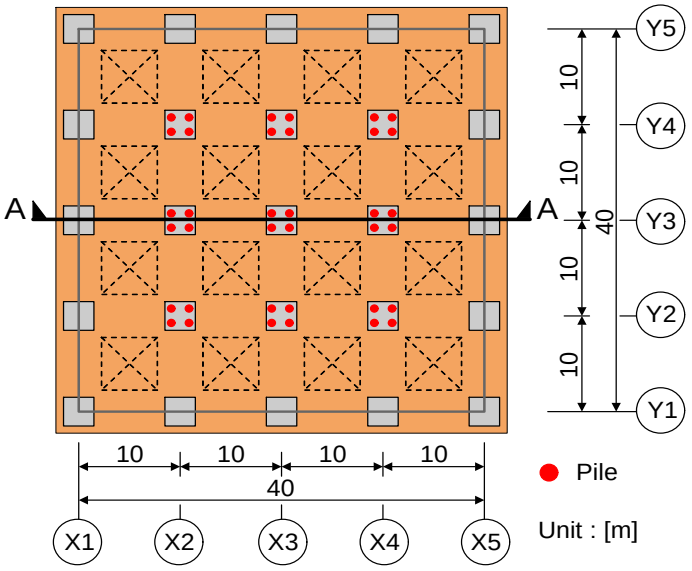

Figure 10. Plan view of Piled TNF (n = 9 × 4)

Fig. 11 shows the calculated deformation of a Piled TNF system (Case 09: D = 0.6 m, L = 25 m, n = 9×4). It is seen that dish-shaped deformation of the TNF occurred.

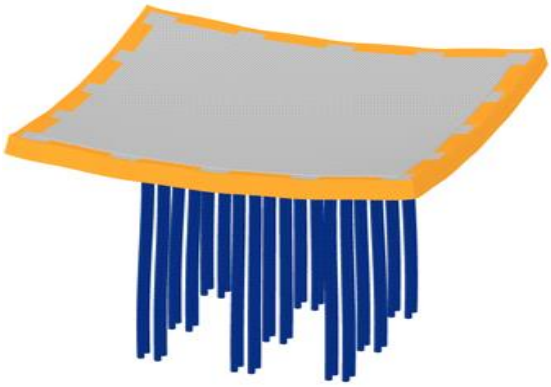

Figure 11. Calculated deformation of Piled TNF (Case 09)

Fig. 12 shows the calculated distributions of vertical displacements of the slab and the ground along Section A-A (see Fig. 10).

Fig. 13 shows the calculated distributions of relative displacements of the slab along Section A-A (see Fig. 10). Here, the relative displacement is defined as the difference between displacements at a given point and at the edge in Section A - A.

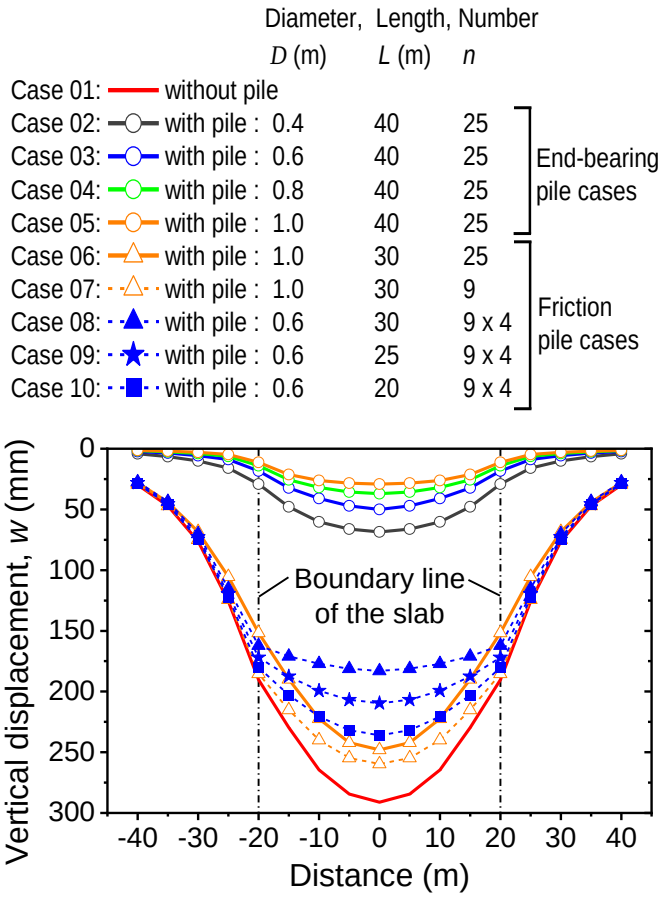

Figure 12. Calculated distributions of vertical displacements of the slab and the ground along Section A - A

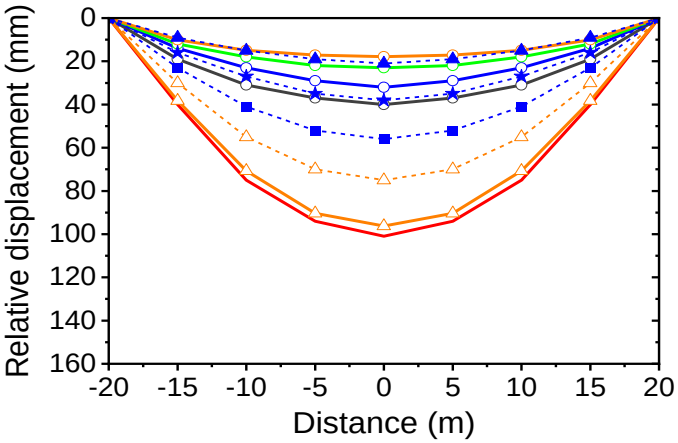

Figure 13. Calculated distributions of relative displacements of the slab along Section A – A

It is seen from Figs. 12 and 13 that the displacements and the differential displacement in the end-bearing pile cases (Cases 02 to 05) are much lower than those in Case 01. The differential displacement in the friction pile cases with the small centered friction pile group (Cases 08 and 09) is comparable to those in the end-bearing pile cases (see Fig. 13).

Fig. 14 shows the distributions of inclination angle of the slab along Section A - A. It is seen that the inclination angles in all end-bearing pile cases except Case 02 are less than the limit value of 3.5×10^{-3} rad specified in The Building Center of Japan (2019).

Fig. 15 shows the distribution of axial forces of center piles. Fig. 16 shows the corresponding distributions of axial stresses.

The axial stress of the center pile exceeds the allowable compressive stress of pile σ_{pa} (= 24 MPa) in Case 02 (D = 0.4 m) and is nearly equal to σ_{pa} in Case 03 (D = 0.6 m) (see Fig. 16). Hence, Case 04 (D = 0.8 m) and Case 05 (D = 1.0 m) are acceptable in the case of the end-bearing pile.

It can be seen from Fig. 16 that the axial stresses of the center piles in all the friction pile cases are less than σ_{pa}.

Let us return to Fig. 14. The inclination angles in Case 07 (n = 9) are less than those in Case 06 (n = 25). Note that D and L are the same in both cases. The Piled TNF with the small centered friction pile group is an efficient foundation system for reducing the differential displacement than the fully Piled TNF, as advocated by Horikoshi and Randolph (1996) for piled rafts.

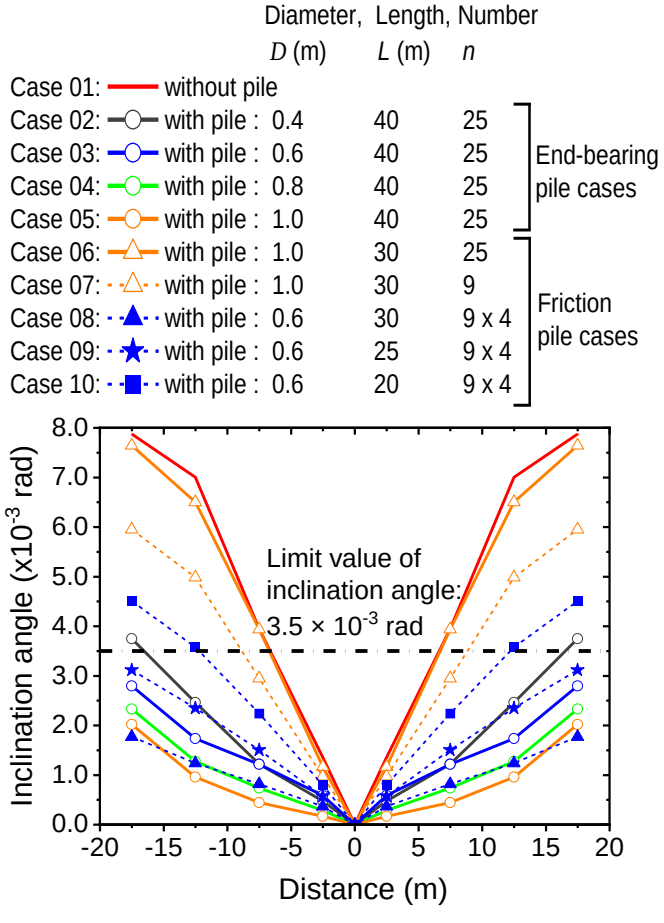

Figure 14. Distributions of the inclination angle along Section A - A

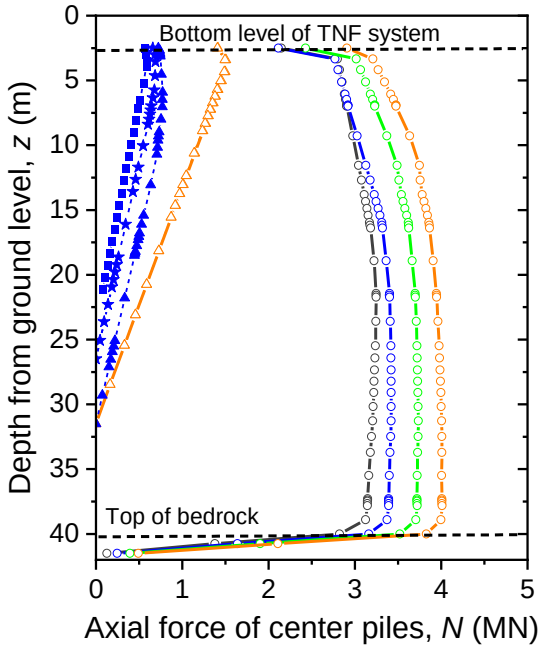

Figure 15. Axial force of the center piles

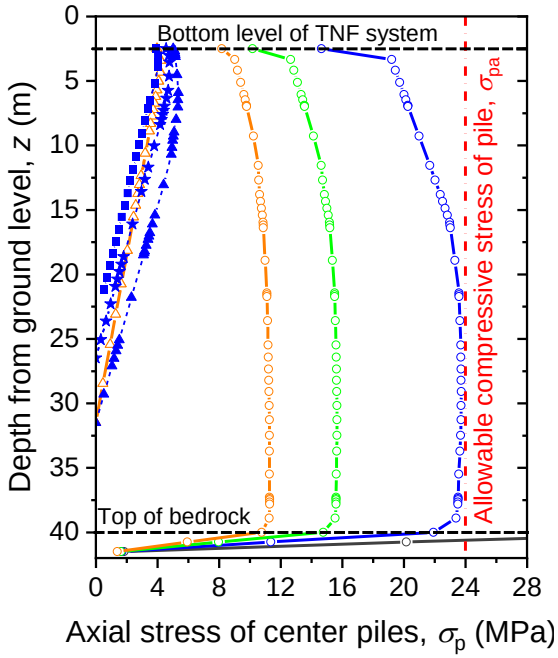

Figure 16. Axial stress of the center piles

However, the inclination angle of Case 07 still exceeds the limit value (see Fig. 14).

The inclination angles in Case 08 are much less than those in Case 07 and less than the limit value. Note that L = 30 m in both cases. As mentioned earlier, one large-diameter pile (D = 1.0 m) is arranged below nine concrete footings in Case 07, while four slender piles (D = 0.6 m) are arranged below nine concrete footings in Case 08 (see Fig. 10).

To find an efficient pile length, analyses of Case 09 (L = 25 m) and Case 10 (L = 20 m) were conducted. It is seen from Fig. 14 that Case 09 is an efficient foundation for reducing the inclination angle.

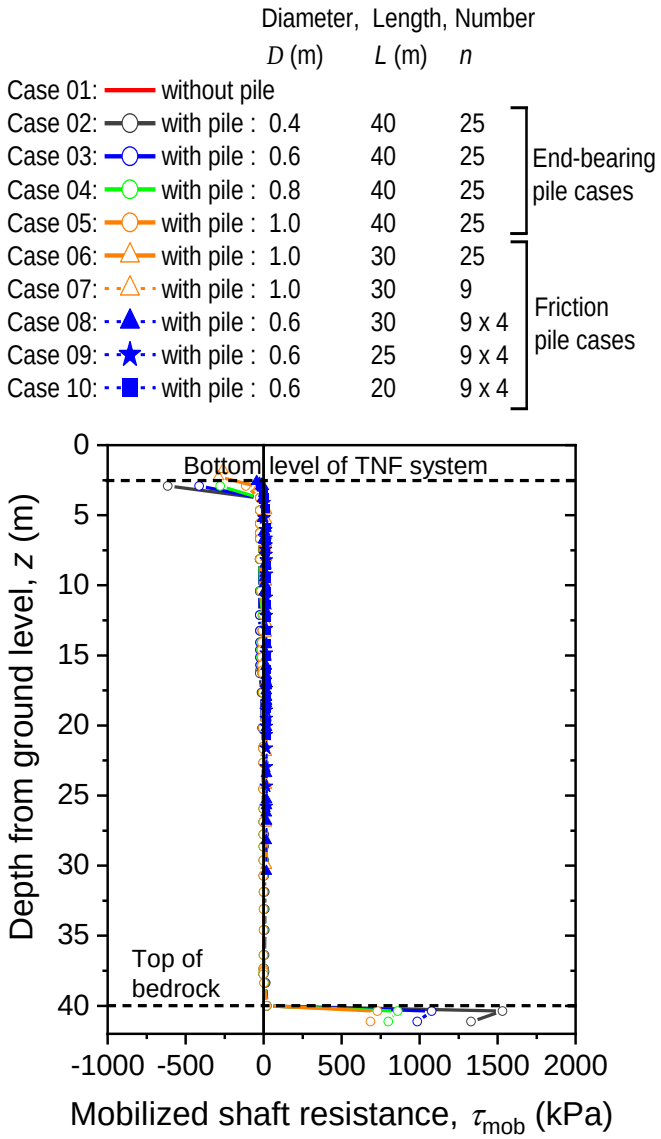

Figure 17. Mobilized shaft resistance

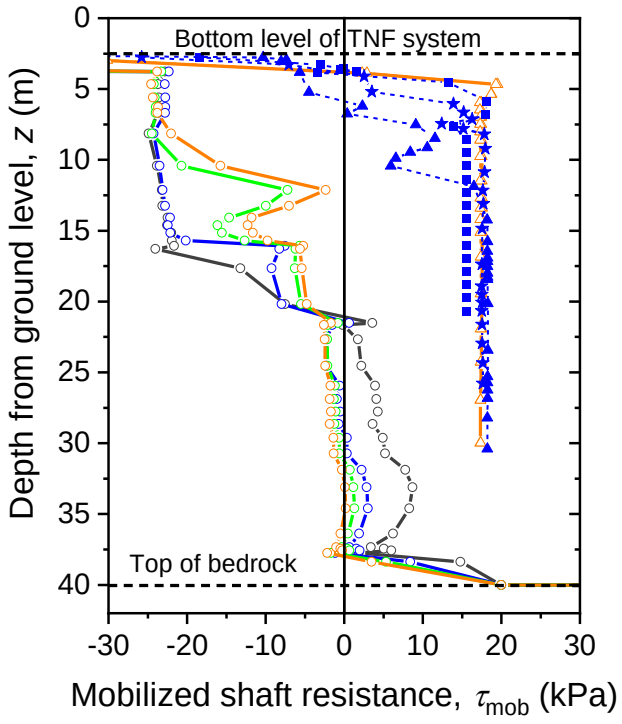

Figure 18. Mobilized shaft resistance (zoom-up)

Fig. 17 shows the mobilized shaft resistance τ_{mob} of the center piles due to the vertical loads of the 5-story building. Zoom-up of the τ_{mob} is shown in Fig. 18. It is seen from Fig. 18 that the value of τ_{mob} has a big difference between the end-bearing pile cases and the friction pile cases. In the end-bearing pile cases (Cases 02 to 05), large τ_{mob} occurs below the depth of 40 m in the bedrock, while negative τ_{mob} occurs at depths up to 22 m, and positive but small τ_{mob} occurs from 22 m to 36 m. In contrast, in the friction pile cases (Cases 06 to 10), the τ_{mob} reaches nearly 20 kPa which is equal to the undrained shear strength c_u of the soft ground below the depth of 12 m.

Let us look back to Figs. 13 and 14. As mentioned earlier, the differential displacement in the friction pile cases with the small centered friction pile group (Cases 08 and 09) is comparable to those in the end-bearing pile cases. It is seen from Fig. 18 that the mobilized shaft resistance τ_{mob} is very small or even negative in the end-bearing pile cases, while τ_{mob} reaches the maximum shaft resistance τ_f = 20 kPa along almost the whole length of the pile. Namely, the friction piles work as displacement reducers, resulting in small differential displacements.

Fig. 19 shows the loads of raft (TNF) and piles vs vertical displacement w at the center of the foundation system in three cases: Case 01 (Unpiled TNF), Case 04 (end-bearing pile case), and Case 09 (friction pile case). R_{raft} is load supported by the raft, and R_{piles} is load supported by the piles.

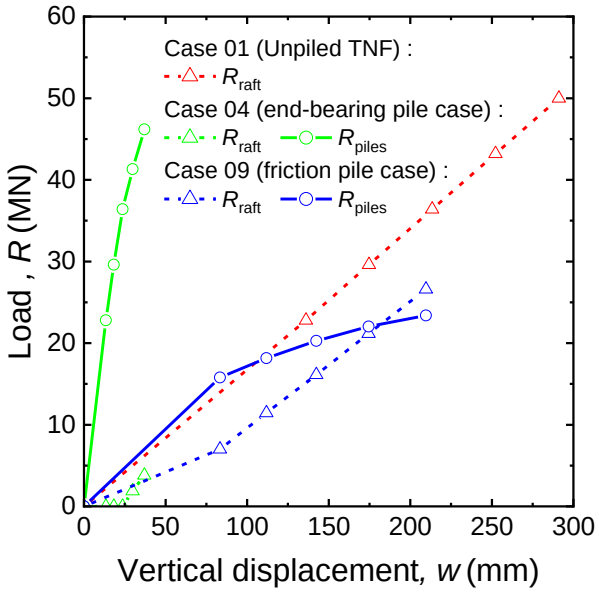

Figure 19. Loads of raft (TNF) and piles vs w

In Case 01, the vertical displacement w is too large because all vertical load F_v is supported by the raft alone. In Case 04, the w is much

suppressed, however, the raft load is very small until w attains 25 mm. In Case 09, although the w is larger than in Case 04, the role of the raft in supporting F_v is much larger.

Fig. 20 shows the load sharing ratio of raft and piles vs vertical displacement w at the center of the foundation system.

In Case 09, the load sharing ratio of the piles decreases with increasing w, and about 50% at the w = 220 mm (subjected to the load of 5-story building). In other words, the load sharing ratio of the raft also attains to 50%. This situation seems to be favorable because both the raft and the piles support F_v efficiently.

In the Building Center of Japan (2019), the allowable maximum vertical displacement is specified as 200 mm for raft foundations. According to this specification, the Piled TNF (Case 09: D = 0.6 m, n = 9×4, L = 25 m) can be applied to 4-story building. It is noticed that the Piled TNF (Case 08: D = 0.6 m, n = 9×4, L = 30 m) can be applied to the 5-story building because the maximum vertical displacement in Piled TNF (Case 08) is 183 mm as shown in Fig. 12.

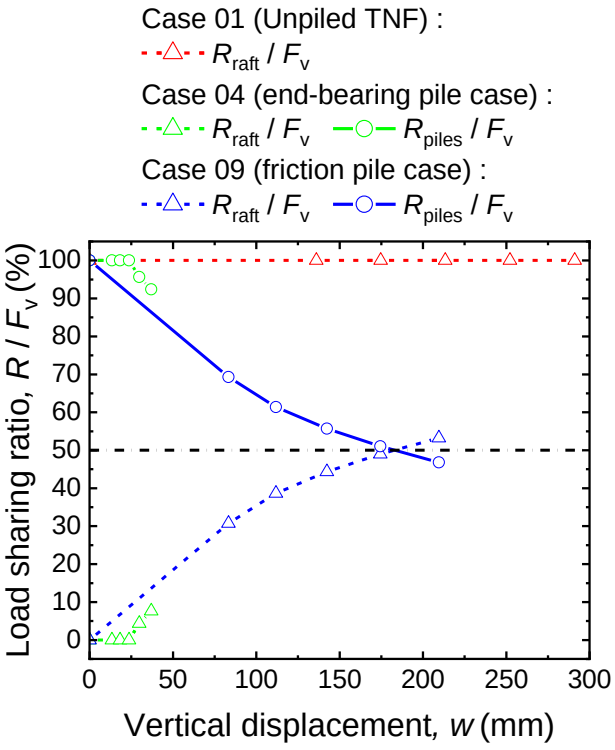

Figure 20. Load sharing of raft (TNF) and piles vs w

4. CONCLUSIONS

In this paper, numerical analyses of behaviors of vertically-loaded Unpiled TNF and Piled TNFs on very soft ground were carried out aiming at reducing differential displacement as well as average displacement.

First, the FEM analysis of the Unpiled TNF was conducted to estimate the vertical load-displacement relation. It was demonstrated that the bearing capacity of the Unpiled TNF was enough for the vertical load of a 5-story building. However, excessive differential displacement occurred.

Hence, then FEM analyses of Piled TNF supported by various combinations of pile diameters, pile lengths, pile numbers, and arrangements were conducted. Main findings from this paper are summarized as follows:

1) The Piled TNF with the small centered friction pile group is an efficient foundation system for reducing the differential displacement compared to the Unpiled TNF and the fully Piled TNF.

2) The differential displacement in the friction pile cases with the small centered friction pile group is comparable to those in the end-bearing pile cases.

3) In the Piled TNF with the small centered friction pile group, both the raft and the piles support vertical load efficiently compared to the end-bearing pile cases.

5. REFERENCES

Bentley (2022): PLAXIS 3D – Manuals.

Briaud, J. L. & Jeanjean, P. (1994). Load Settlement Curve Method for Spread Footings on Sand and Horizontal Deformations of Foundations and Embankments. *ASCE Journal of the Geotech. Eng. Division*, 2, pp 1774-1804.

Cong, H.V., Takeuchi, K., Vakilazad, A. & Matsumoto, T. (2022). Parametric numerical study on deformation of the Tender Net Foundation subjected to vertical loading. *The 11th International Conference on Stress Wave Theory and Design and Testing Methods for Deep Foundations*, Rotterdam, the Netherlands, 6p., DOI 10.5281/zenodo.7142087.

Horikoshi, K. & Randolph, M. F. (1996). Centrifuge modelling of piled raft foundations on clay. *Géotechnique*, 46(4), pp 741-752.

The Building Center of Japan (2018). Guidelines for design and quality control of soil improvement - Deep or shallow mixing treatment method using cement-based solidifying materials. ISBN978-4-88910-174-4 (in Japanese).

The Building Center of Japan (2019). Recommendations for design of building foundations. ISBN978-4-8189-0652-5 C3052 (in Japanese).